OPEN ACCESS International Journal of Applied Biology

ISSN : 2580-2410
eISSN : 2580-2119

Physico-chemical Characterization of Biochar from Selected Ligno-cellulosic Biomass for The Sustainable Utilization

Anjali T. B[1], Anand M[1*], Akhilesh K. B[1], Madhuraj P.K[1], Ratheesh Kumar C.S[1], Archana Waran[1]

[1] School of Environmental Studies, Cochin University of Science and Technology, Cochin, Kerala, India

Abstract

Biochar is a thermal decomposition product known to mitigate climate change and a supplement to enhance soil fertility. The fine-grained, highly porous structure of biochar makes it a popular choice in environmental research. This study aims to assess the Physico-chemical properties and morphological changes in the biochar prepared from feedstocks: sawdust, sugarcane bagasse, and soapnut pith of Sapindus trifoliatus, native to the foothills of Western Ghats, Kerala, at a temperature of 300°C and 600°C with 30 minutes residence time. The pyrolytic temperature and feedstock type may affect the yield, ash content, volatile matter (VM), fixed carbon (FC), and nutrient composition of biochar. The selection of these two factors is critical before proceeding with charring. The efficiency of biochar was determined through proximate, ultimate, and morphological characterizations. The pH of high-temperature biochar (sawdust biochar, sugarcane bagasse biochar, and soapnut pith biochar prepared at 600°C) was more alkaline (≥7) compared with low-temperature ones. The char yield was highest at 300°C, whereas the fixed carbon was limited. The VM/FC ratio of SDB600 at 1.09±2.3 represents the highest aromaticity and long-term stability. Therefore, SDB600 can be recommended for soil supplementation purposes. The macrospores were uniformly distributed throughout the biochar surface. Sugarcane bagasse pyrolyzed at 600°C (SBB600) possessed the minimum pore diameter (0.87-9.17µm), with the highest surface area; so that it could be an optimum habitat for soil microbiota as well as a suitable adsorbent for environmental remediation applications. The study suggests that biochar made from these ligno-cellulosic feedstocks is a sustainable tool and a value-added product for environmental management.

Article History
Received September 29, 2022
Accepted December 14, 2022

Keyword
Biochar;
Carbon sequestration;
Ligno-cellulosic feedstock;
Macropore;
Pyrolysis

Introduction

Ligno-cellulosic biomass or plant dry matter is a widely used feedstock for biofuel production (e.g., ethanol) due to its abundance. It comprises carbohydrate polymers such as cellulose, hemicelluloses, and lignin. The tight bond between different sugar monomers (six and five-carbon sugars) and lignin resulted in the formation of lignocellulosic biomass belonging to three classes, namely, virgin biomass, waste biomass, and energy crops. The naturally occurring terrestrial plants such as trees, bushes, and grass belong to the class of

CONTACT : ANAND M anandm@cusat.ac.in

virgin biomass (Sushil A. et al., 2018). In contrast, waste biomass is a low-value byproduct of various industrial sectors, including agriculture (corn stover, sugarcane bagasse, straw, etc.) and forestry (sawmill and paper mill discards). The high-yield ligno-cellulosic biomass like switch grasses (*Panicum virgatum*), elephant grass, and sugarcane bagasse are examples of energy crops that serve as raw materials for producing bio-energy and other value-added products. The lingo-cellulosic biomass consists of 15%-25% lignin, 35%-55% cellulose, 25%-40% hemicelluloses, and a small percentage of extractives, protein, and ash (Sushil A. *et al.,* 2018).

Agricultural residues are readily available, inexpensive renewable lingo-cellulosic fiber resources with a structure, composition, and properties similar to other plant fibers (McMichael *et al.,* 2007). Its prominent examples include wheat, rice, barley straw, corn stover, sorghum stalks, coconut husks, sugarcane bagasse, pineapple, and banana leaves. The heating value of agricultural biomass generally ranges from 12 to 20 M J/kg and is dependent on the ash content (Sushil A. *et al.,* 2018). The elemental compositions of wood residues contain a little higher carbon and hydrogen than agricultural residues. Crop residues include field and process residues (Horisawa *et al.,* 1999). The field residues are the leftover materials like stalks and stubble (stems), leaves, and seed pods. The process residues are materials left after processing the crop into a usable resource. These residues include husks, seeds, bagasse, molasses, and roots, used as animal fodder, soil amendment, and fertilizers. The complexity and variability of feedstocks pose many challenges in waste-to-energy processes. Technically, the amount of moisture in a feedstock limits the conversion pathway for producing biofuels, bioproducts, and biopower. Thermochemical conversion technologies are preferred to dry feedstocks (< 50% moisture) with well-understood material and preparation costs (Duchan & Kopar, 2001).

This study aimed to prepare and characterize a value-added product called biochar from varieties of lingo-cellulosic biomass such as sawdust, sugarcane bagasse, and soapnut pith fibers after pyrolyzed at 300 and 600^{o}C temperature with a residence time of 30 minutes. Sawdust is a processed hardwood biomass residue obtained from the timber industry. It possesses the firing capacity and is a fuel source in thermal processes (Demir, 2008; Low, Fazio, & Guite, 1984). The elemental composition of sawdust includes carbon (60.8%), hydrogen (5.2%), oxygen (33.8%), and nitrogen (0.9%) (Horisawa *et al.,* 1999). Sugarcane bagasse is a fibrous agriculture residue that remains after crushing the stalks to extract juice for sugar and jaggery production. It is the raw material for heat production, manufacturing pulp, and building materials. Sugarcane bagasse is readily available in small-scale jaggery units in Kerala.

The soapnut pith is one of the residues procured from soapnut fruit at the end of saponin extraction. It mainly consists of the outermost fibers shell residues of soapnut (*Sapindus trifoliatus*). *Sapindus trifoliatus* is a small tree commonly available in tropical and temperate regions, especially in the foothills of the Western Ghats and Eastern Ghats (Chopra RN et al., 1956). The fruit is mainly used for preparing hair tonics, cosmetics, skin creams, and anti-spermatic activity. The *Sapindus trifoliatus* is widespread in South India ("soapnut tree of South India"), where the climate is warmer and milder (Publication and Informative Directorate, 1988). Saponin from soapnut is also widely used in the native medicine and pharmaceutical industries (Robber JM and Tyler VS, 1996), used as detergents (Edeoga HO et al., 2006), and used for environmental remediation (Urum K and Pekdemir T., 2004). Recent studies are on progress to evaluate the soapnut oil as a potential source for biodiesel, and bio inhibitor, whereas oil cake obtained after the extraction of oil can be used as bio-manure, bioherbicide, bio-fungicide, and biopesticide. Soapnut pith is the residue obtained after the extraction of soapnut juice. The studies related to the thermal conversion of such residues are scarce.

Pyrolysis is one of the thermal conversion processes that produces a carbon-rich product called biochar. Previous studies have investigated the properties of a variety of feedstock-derived biochar, except the agricultural residues of *sapindus trifoliatus*, hardwoods, and sugarcane from the foothills of Western Ghats Kerala. Biochar possesses enormous physicochemical advancement over feedstock due to pyrolysis. This work finds out the possible physical, chemical, and morphological advancement in the biochar from three distinct biomass materials such as hardwood sawdust, sugarcane bagasse, and soapnut pith of *Sapindus trifoliatus* native to Kerala. This study also aimed to identify the best biochar for cultivable soil as a supplement, a suitable adsorbent for environmental remediation based on their characteristic features.

Materials and Methods

Pyrolysis is one of the thermochemical techniques opted for biochar production in this study. It is the thermochemical conversion of biomass under a limited oxygen supply in a laboratory muffle furnace. The analytical part uses instruments such as the CHNS elemental analyzer, FTIR (Fourier Transform Infra-Red) spectroscopy for functional group identification and Scanning Electron Microscope-Energy Dispersive X-ray Analyzer (SEM-EDAX) for structural characterization studies.

Feedstock Collection and characterization

The biochar was prepared from Sawdust (SD), Sugarcane Bagasse (SB), and Soapnut Pith (SP) of *Sapindus trifoliatus* (Figure 1). Around 5 Kg of processed hardwood Sawdust was collected from a nearby timber industry. Sugarcane bagasse was collected in bulk from the small-scale jaggery production units. Locally available soapnut, *sapindus trifoliatus* was crushed and squeezed to remove the juicy matter and collect the fibrous pith. These feedstocks were air-dried at room temperature for two days, then crushed and later stored in air-tight polythene bags for characterization studies.

Figure No.1 Different Ligno-cellulosic biomass collected for biochar production, (a) Sawdust (SD), (b) Soapnut Pith (SP), (c) Sugarcane Bagasse (SB).

Preparation of Biochar

The thermochemical conversion of feedstock into biochar was performed in a Laboratory Muffle furnace to optimize the pyrolysis conditions. 50 g of air-dried and chopped feedstock materials were accurately weighed in silica crucibles and pyrolyzed under oxygen-limited conditions at two different temperatures with 60 minutes of residence time. The feedstock was pyrolyzed at low (300°C) and high temperatures (600°C). The prepared biochar samples were ground, passed through a 2mm sieve, cooled in desiccators, and used for further analysis.

Characterization of Biochar

The proximate, ultimate, and surface morphological parameters were analyzed to determine the temperature influence of different ligno-cellulosic biochar materials in their Physico-chemical and structural properties based on the ASTM D5142 methods. The proximate biochar analysis comprises; Bulk density (gcm^{-3}), Moisture content (%), Ash content (%), Volatile matter (%), Biochar yield (%), and Fixed Carbon (%).
The bulk density (gcm^{-3}) has been identified by the methodology described by Masulili et al., 2016, based on the equation as follows:

$$\textbf{Bulk density}\left(\frac{\mathbf{g}}{\mathbf{cm^3}}\right)=\textbf{Weight of oven dried biochar}(\mathbf{g})/\textbf{The volume of the packed materials }(\mathbf{cm^3})$$

The presence of moisture content in the biochar was measured following the methods described by Masulili (2010), and the equation for calculating the moisture content is as follows,

$$\textbf{Moisture Content }(\%)=\frac{\textbf{Initail weight of Biochar }(\mathbf{g})-\textbf{Oven dry weight}(\mathbf{g})}{\textbf{Oven dry weight }(\mathbf{g})}*\mathbf{100}$$

The volatile matter emitted from the feedstock during the pyrolysis has been identified based on the methodology described by Shi-Xiang Z.*et al.,*2017. The formula for calculating the volatile matter (%) is given below.

$$\textbf{Volatile matter }(\%)=\frac{\mathbf{W_1}-\mathbf{W_2}}{\mathbf{W_3}}*\mathbf{100}$$

W_1= weight of sample and crucible before heating (gm)
W_2= weight of a given sample (gm)
W_3= weight of sample and crucible after heating

The biochar yield was analyzed by a method derived by Sadaka *et al.,* 2014. The equation for calculating the yield (%) is as follows:

$$\textbf{Yield }(\%)=\textbf{Mass of biochar }(\mathbf{g})*\textbf{100 Oven dry mass of feedstock }(\mathbf{g})$$

The fixed carbon content in the biochar samples was determined by the formula mentioned by Novak *et al.,* 2009.

$$\textbf{Fixed Carbon }(\%)=\mathbf{100}-(\textbf{Ash }\%+\textbf{VM }\%)$$

The ultimate parameters include pH, electrical conductivity (EC), elemental carbon, hydrogen, nitrogen, and Sulphur. After the pH and conductivity meter calibration, readings were (Rajkovich *et al.,* 2011). The moisture content of prepared biochar material was analyzed by the methodology described by Maiti S K., 2003.

Elemental Analysis

The elemental compositions in the raw sawdust, sugarcane bagasse, soapnut pith, and biochar particles were determined using the CHNS ELEMENTAR Vario EL III analyzer available in the Sophisticated Test and Instrumentations Centre (STIC), Cochin University of Science and Technology, Cochin.

Scanning Electron Microscope- Energy Dispersive X-Ray Analysis (SEM- EDAX)

SEM-EDAX is one of the best analytical methods for examining biochar materials' surface morphological changes and atomic compositions. The instrument used in this study was a Scanning Electron Microscope - Energy Dispersive X-ray Spectroscope model Jeol 6390LA/ OXFORD XMX N under 2µm and 10 µm resolutions.

Fourier Transform Infrared Spectroscopy (FTIR) Analysis

FTIR is an analytical instrument for functional group identifications in organic materials like biochar. The sample has been analyzed in the Shimadzu FTIR Spectrometer facility at the School of Environmental Sciences, Mahatma Gandhi University, Kottayam. The software, KnowItAll is used for functional group identification based on spectral similarities.

Statistical Analysis

Statistical analysis of data was conducted using *ORIGINPRO*® software and *Microsoft Excel 2010*®. The Two-Way ANOVA was conducted to find out whether there is an interaction between feedstock and pyrolysis temperature on physical and chemical parameters. Further, in the case of significant results, the Tukey's Honestly-Significant-Difference (Tukey HSD) test was performed to determine the groups between which there exist significant differences ($p=0.05$).

Results and Discussion

Statistical Analysis

The elemental composition of sawdust, sugarcane bagasse, and soapnut pith are depicted in Table 1. The weight percentage of Carbon and Sulphur was higher in sawdust biomass (44.13% and 0.17%) than in sugarcane bagasse and soapnut pith. The elemental hydrogen and nitrogen were high in soapnut pith (10.65% and 1.93%), followed by sugarcane bagasse and sawdust. These visible changes in the elemental compositions of the feedstock have been reflected in their H/C and C/N ratios. As a result of high carbon and low nitrogen content in sawdust biomass, the carbon to nitrogen ratio (105.07) was most elevated. In contrast, the soapnut pith's high hydrogen and low carbon contents exhibit maximum hydrogen to carbon ratio (0.246).

Table 1. Elemental compositions of Ligno-cellulosic biomasses include Sawdust, Sugarcane bagasse, and Soapnut pith.

	Elemental Compositions						
Feedstock	**Sample Code**	**C (%)**	**H (%)**	**N (%)**	**S (%)**	**H/C**	**C/N**
Sawdust	SD	44.13	4.13	0.42	0.17	0.093	105.07
Sugarcane Bagasse	SB	40.40	6.17	0.89	ND	0.152	45.39
Soapnut Pith	SP	43.17	10.65	1.93	0.01	0.246	22.36

Functional Groups in the Feedstock and Biochar

The FTIR spectrum provided the entire bond information in a molecule based on its vibration and rotational motion. The FTIR spectroscopy investigates the functional groups existing in the feedstock and biochar. The profile of FTIR spectra obtained from different ligno-cellulosic biomass and its derived biochar samples are shown in figure 2.

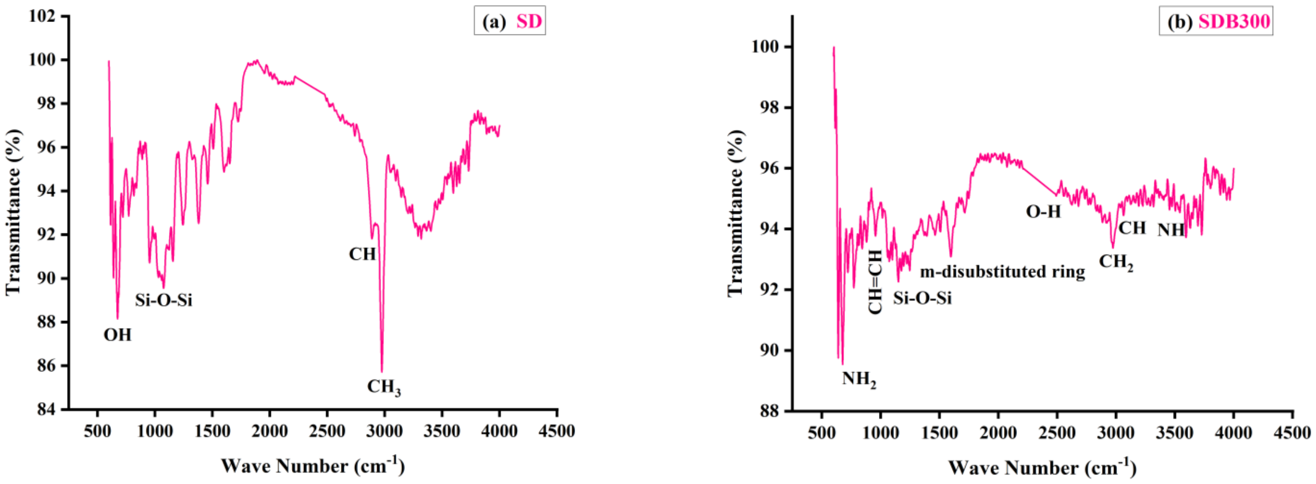

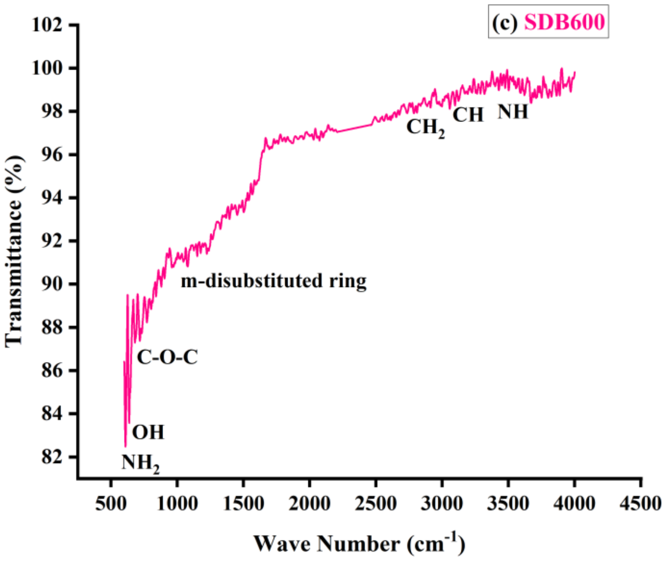
(c) SDB600
Transmittance (%)
102
100
98
96
94
92
90
88
86
84
82
500
1000
1500
2000
2500
3000
3500
4000
4500
Wave Number (cm-1)
NH2
OH
C-O-C
m-disubstituted ring
CH2
CH
NH

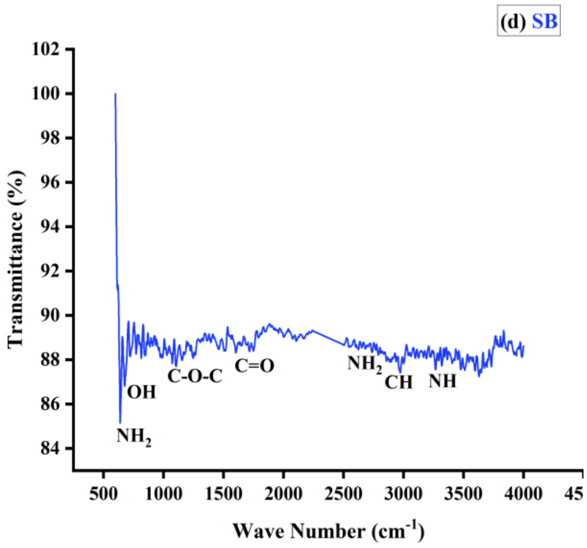
(d) SB
Transmittance (%)
102
100
98
96
94
92
90
88
86
84
500
1000
1500
2000
2500
3000
3500
4000
45
Wave Number (cm-1)
NH2
OH
C-O-C
C=O
NH2
CH
NH

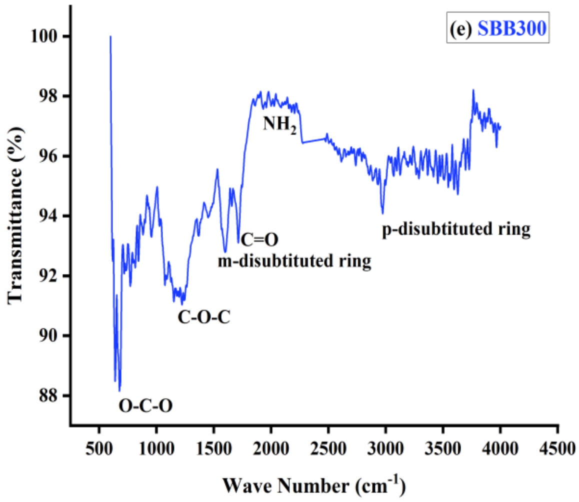
(e) SBB300
Transmittance (%)
100
98
96
94
92
90
88
500
1000
1500
2000
2500
3000
3500
4000
4500
Wave Number (cm-1)
O-C-O
C-O-C
C=O
m-disubtituted ring
NH2
p-disubtituted ring

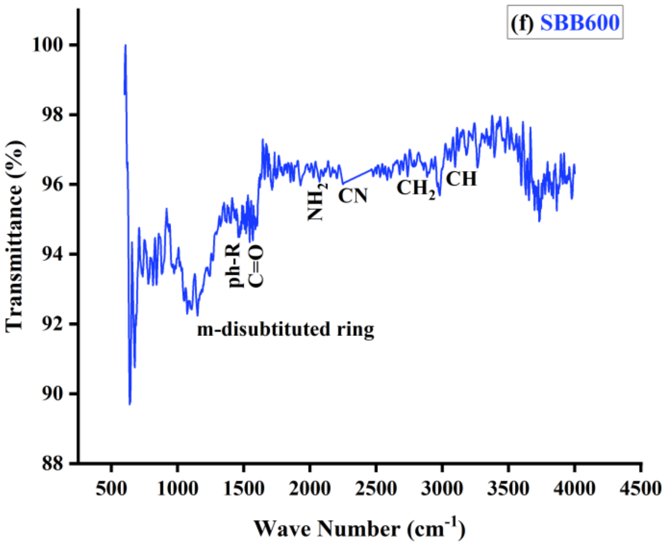
(f) SBB600
Transmittance (%)
100
98
96
94
92
90
88
500
1000
1500
2000
2500
3000
3500
4000
4500
Wave Number (cm-1)
m-disubtituted ring
ph-R
C=O
NH2
CN
CH2
CH

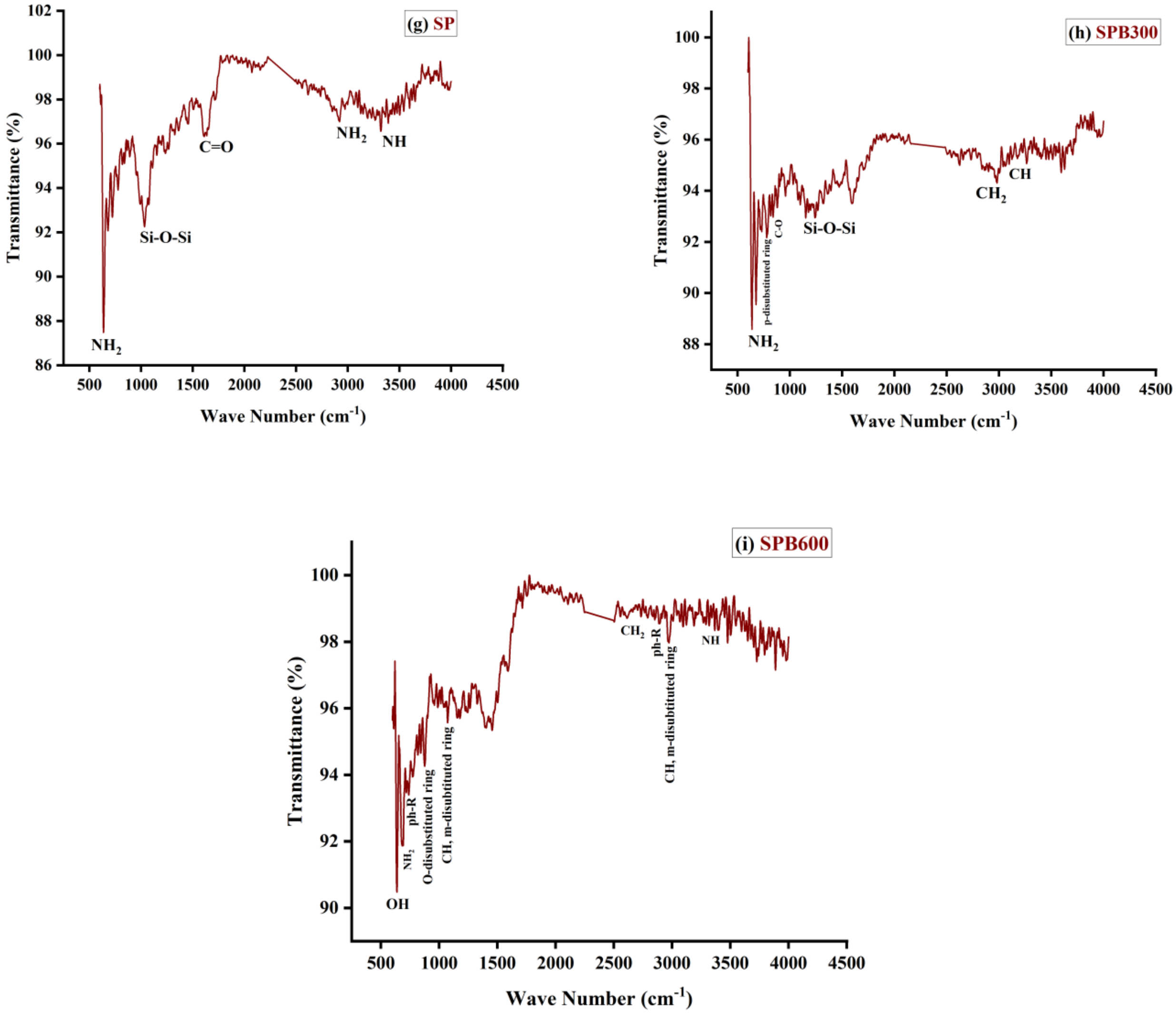

Figure 2. FTIR spectra of feedstock biomass and biochar samples: (a) Sawdust, (b)SDB300, (c)SDB600, (d) Sugarcane bagasse, (e)SBB300, (f)SBB600, (g) Soapnut pith, (h)SPB300, and (i)SPB600.

The FTIR spectra of feedstock sawdust and sugarcane bagasse exhibited two similar functional groups. The peaks around 675.09 cm^{-1} corresponded to the strong stretching mode of vibrations of the O-H functional group belonging to cellulose and derivatives classification. The peaks around 2887.44 cm^{-1} corresponded to weak stretching of C-H; similarly, sawdust and soapnut pith showed a strong stretching of the Si-O-Si bond at the peak around 1033.86 cm^{-1} to the class silicones. The FTIR peak obtained around 638.44 cm^{-1} corresponded to the medium deformation of the NH_2 functional group under the classification polyamides were common for the feedstock sugarcane bagasse and soapnut pith. The biochar samples prepared at 300°C exhibited the presence of m-disubstituted and p-disubstituted aromatic ring structured polymers with C-H bond between the wavelength 1590-1625cm^{-1} and 3050-2070 cm^{-1}. Whereas, the high temperature biochar prepared at 600°C shows weak stretching of CH (1085-1105cm^{-1} and 3010-3079cm^{-1}) and Ph-R bonds (1590-1615cm^{-1}, 3070-3095cm^{-1} and 730-770cm^{-1}) of aromatic polyesters. The FTIR peaks have shown the existence of more aromatic functional groups in SPB600 compared to the feedstock and the rest of the biochar samples. High-temperature biochar's aromatic nature can contribute to long-term soil stability and exist as a non-labile carbon source.

The pyrolysis temperature is more critical than residence time for the specificity of functional groups. The existing literature shows that the functional groups in biochars from lignin-rich feedstock are more temperature resistant (Janu R. *et al.,* 2021). In a study by Janu R. et al., 2021, the infrared spectra of biochars produced at 300°C and 450 °C were similar. In contrast, a pyrolysis temperature of 600 °C led to a partial loss of biochar surface functional groups. The wave number ranges between 2920-2885 cm-1 (C-H stretching) were assigned to aliphatic functional groups. The strong band at 1030 cm^{-1} is due to the C-O stretching and is associated with the oxygenated functional group of cellulose, hemicelluloses, and methoxyl group of lignin. The intense band at 1270 cm^{-1} was assigned to phenolic O-H groups (Domingues RR. *et al.,* 2017). The appearance of more aromatic chemical bonds is attributed to an increasing degree of condensation of the organic biochar compounds along with an increase in the pyrolysis temperature (Keiluweit *et al.,* (2010), Jindo *et al.,* (2014), Melo *et al.,* (2013)). The higher temperatures also promote the structural ordering of biochar, resulting in larger aromatic ring clusters (Morin *et al.,* 2016). According to advanced characterization techniques, the literature agrees that a high pyrolysis temperature promotes the loss of functional groups and the growth of aromatic ring systems (Asadullah, M. *et al.,* 2010).

Biochar Characterization

The proximate and ultimate analysis represents biochar's physical and chemical properties prepared at conducible temperature conditions. The pyrolysis temperature and the feedstock type can interfere with biochar's Physico-chemical and structural properties.

Proximate parameters

The proximate analysis results of biochar samples are depicted in Table 2. All the biochar particles from different feedstock exhibit textural changes concerning temperature conditions. The pyrolyzing temperature and feedstock type are the fundamental factors for controlling the proximate parameters such as biochar yield, ash content, volatile matter, and fixed carbon content. It was found that the high-temperature biochar possessed higher ash content, fixed carbon, and low volatile matter (Fig.3(a), (c), (b)). The ash content was found to be maximum in the sawdust biochar produced at high temperatures (Table 2) compared to sugarcane bagasse and soapnut pith biochars.

In contrast, the mean difference is statistically significant at the 0.05 level. It is mainly due to the differences in the concentrations of ash-forming elements such as calcium carbonate, potassium silicates, iron, and other metals (Lewandowski and Kicherer 1997). Wei *et al*., 2017 also reported that the biochar ash content gradually increased with an increasing pyrolysis temperature. Similarly, fixed carbon content gradually increased from 300°C to 600°C in sawdust biochar without any significant difference between the means of soapnut pith-derived biochars observed at 300°C to 600°C. This increased fixed carbon content in sawdust biochar may be due to the increased loss of volatile matter (Crombie *et al*., 2013; Sun *et al*., 2017).

Table 2. Proximate parameters of biochar derived from various ligno-cellulosic biomasses such as Sawdust, Sugarcane Bagasse, and Soapnut Pith

Feedstock	Pyrolysis Temperature (°C)	Biochar Sample Code	Proximate Parameters						
			Moisture Content^a (%)	Bulk Density^a (gcm^{-3})	Ash Content^a (%)	Volatile Matter^a (%)	Fixed C^a (%)	Yield^a (%)	VM/FC^b
Sawdust	300 °C	SDB300	1.17±0.11	0.222±0.01	10.80±0.04	76.45±12.25	12.18±1.6	21.36±1.7	6.27±7.6
	600 °C	SDB600	3.12±0.10	0.175±0.05	50.84±0.55	24.05±3.5	21.87±1.5	5.78±0.6	1.09±2.3
Sugarcane Bagasse	300 °C	SBB300	7.22±0.08	0.067±0.01	6.49±0.55	81.71±6.6	5.86±1.4	11.94±0.7	13.94±4.7
	600 °C	SBB600	2.25±0.10	0.069±0.01	11.44±0.81	66.56±4.3	17.41±1.5	1.13±0.5	3.82±2.8
Soapnut Pith	300 °C	SPB300	28.98±0.70	0.393±0.11	6.96±1.25	86.94±4.2	2.16±0.68	27.71±1.8	40.25±6.1
	600 °C	SPB600	5.42±0.21	0.075±0.30	27.44±1.66	64.86±4.0	4.17±0.97	15.51±2.5	15.55±4.1

[a] Values are the average of four replicates ± standard deviation
[b] Volatile matter/Fixed carbon ratio

Generally, the percentage of volatile matter in biochar samples decreased consistently with pyrolysis temperature. Compared to sugarcane bagasse and soapnut pith biochars, a significant difference can be observed in the sawdust biochar produced at 300°C (SDB300) and 600°C (SDB600). The high fractions of volatile content in sawdust biomass are emitted while charring. Sadaka et al., 2014 have reported that the percentage of volatile matter in corn stover (*Zea mayas* L.) biochar decreases with increasing pyrolysis temperature. In the case of bulk density and moisture content, only slight variations were visible, and no statistically significant difference can be observed among the different feedstock-derived biochar.

The volatile matter to fixed carbon ratio (VM/FC) can be used as an indicator for biochar stability in amended soils. The biochar with a VM/FC ratio ranging from 0.5 to 1.0 can be stable in soils (Novak and Busscher 2013). The gradual VM/FC ratio decrease in the biochar samples produced at 600°C may have increased stability and long-term carbon sequestration potential in amended soil. Sawdust biochar (SDB600) made at 600°C had a VM/FC ratio of 1.09±2.3, which exhibits more stability than soapnut pith biochar (SPB600) and sugarcane bagasse biochar (SBB600) with a VM/FC ratio more remarkable than the optimum (fig.3 (e)). The stability of high-temperature biochars decreased in the order SDB600>SBB600>SPB600. At the same time, low-temperature biochars such as SDB300, SBB300, and SPB300 with VM/FC ratio higher than the optimum is more labile and unstable in the amended soil and possess less carbon sequestration potential.

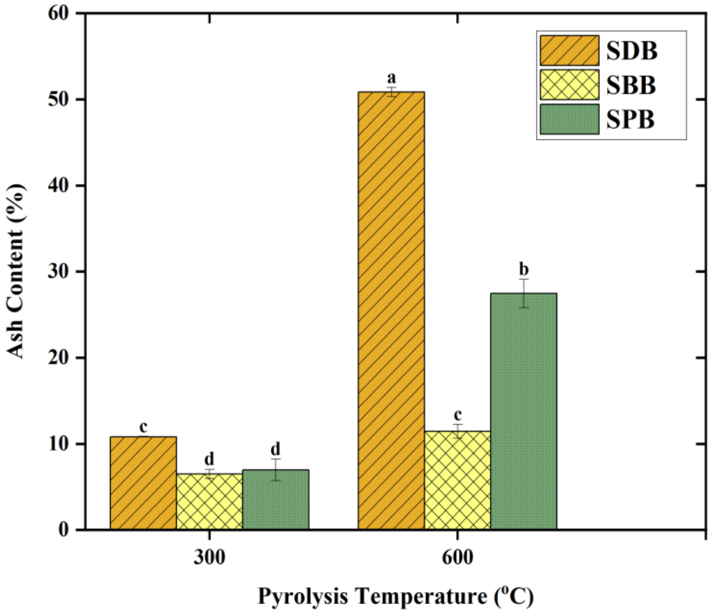

Figure 3 (a) Ash content of the biochar derived from ligno-cellulosic biomasses such as Sawdust, Sugarcane bagasse, and Soapnut pith pyrolyzed at 300°C and 600°C. Data are presented as mean ± std.

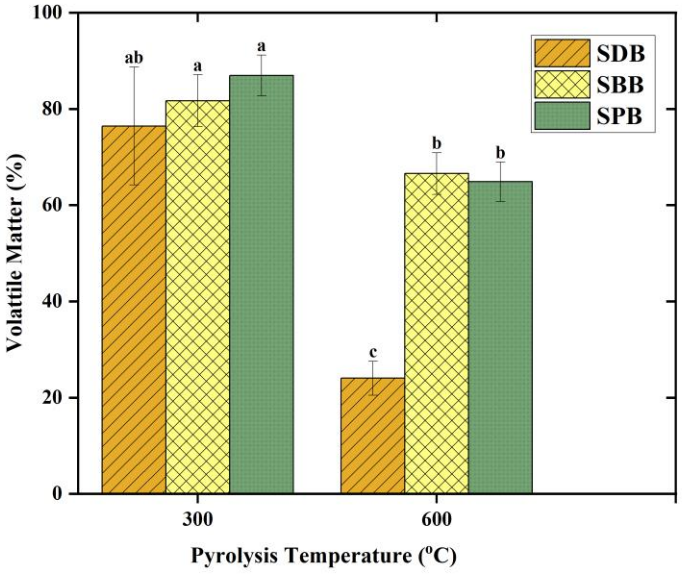

Figure 3 (b) Volatile matter of the biochar derived from ligno-cellulosic biomasses such as Sawdust, Sugarcane bagasse, and Soapnut pith pyrolyzed at 300°C and 600°C. Data are presented as mean ± std.

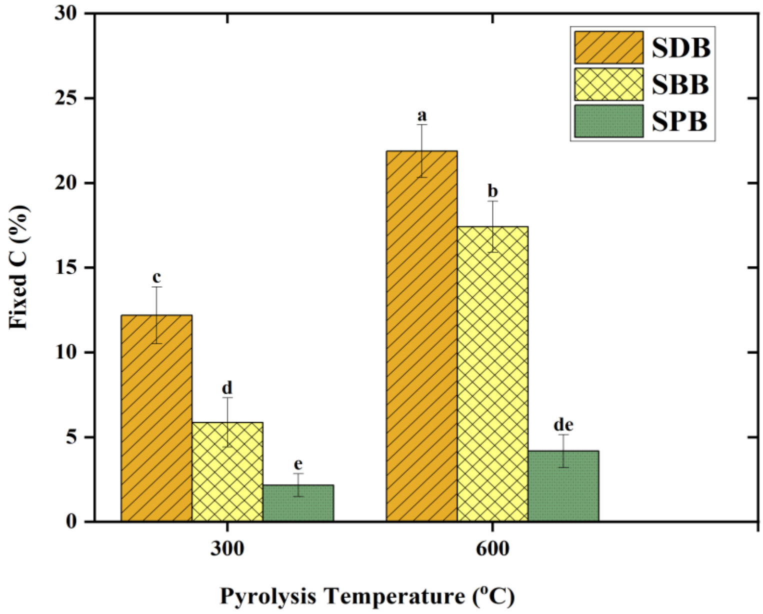

Figure 3 (c) Fixed Carbon of the biochar derived from ligno-cellulosic biomasses such as Sawdust, Sugarcane bagasse, and Soapnut pith pyrolyzed at 300°C and 600°C. Data are presented as mean ± std.

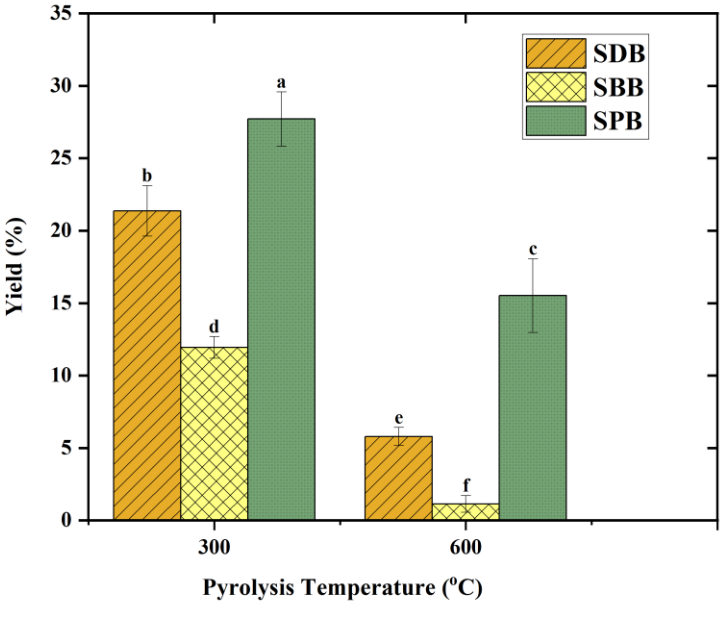

Figure 3 (d) Yield of the biochar derived from ligno-cellulosic biomasses such as Sawdust, Sugarcane bagasse, and Soapnut pith pyrolyzed at 300°C and 600°C. Data are presented as mean ± std.

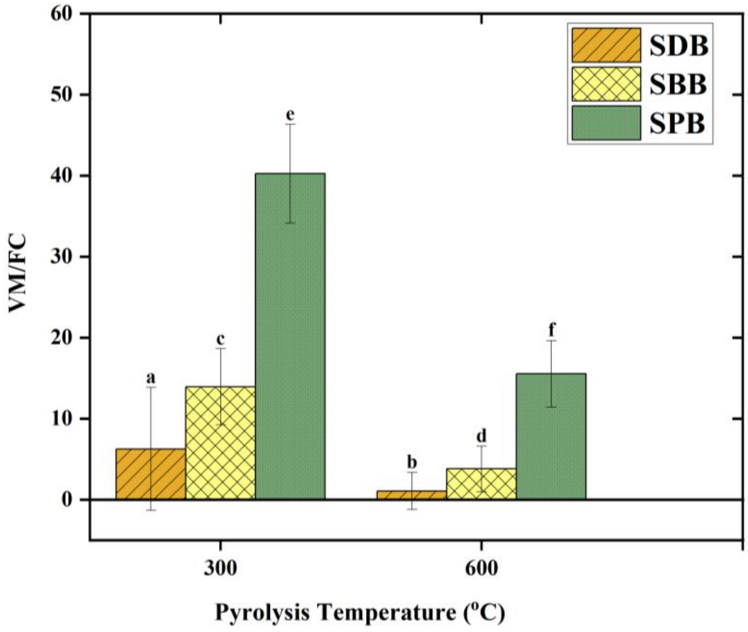

Figure 3 (e) VM/FC ratio of the biochar derived from ligno-cellulosic biomasses such as Sawdust, Sugarcane bagasse, and Soapnut pith pyrolyzed at 300°C and 600°C. Data are presented as mean ± std

Ultimate Parameters

The ultimate parameters are given in Table 3. An interdependent change can be observed in the pH and EC values of each of the biochar samples. The pH was increased with the pyrolysis temperature from 300°C to 600°C. Except for SBB600, high-temperature biochars such as SDB600 and SPB600 possess alkaline pH (i.e., 08.67±0.4 and 09.10±0.2), which helps to neutralize the acidic cultivable soils (fig.4 (a)). Theoretically, the acidic functional groups in feedstock like quinine, chromene, and diketone can be abolished at high temperatures. As a result, biochar after pyrolysis tends to be more alkaline (Mukherjee *et al*., 2011; Tsai 2017).

Table 3. Ultimate parameters of biochar derived from various ligno-cellulosic biomasses such as Sawdust, Sugarcane bagasse, and Soapnut pith.

Feedstock	Pyrolysis Temperature (°C)	Biochar Sample Code	Ultimate Parameters							
			P^H	EC (mS/cm)	C (Wt %)	H (Wt %)	N (Wt %)	S (Wt %)	H/C	C/N
Sawdust	300 °C	SDB300	06.83±0.2	4.42± 0.5	53.5	0.54	1.00	0.0	0.010	53.5
	600 °C	SDB600	08.67±0.4	5.68± 0.4	75.0	1.26	0.45	ND	0.016	166.6
Sugarcane Bagasse	300 °C	SBB300	04.80±0.2	2.88±0.2	57.0	0.51	0.91	0.0	0.008	62.6
	600 °C	SBB600	06.80± 0.7	6.54±0.5	69.1	3.89	0.52	ND	0.056	132.8
Soapnut Pith	300 °C	SPB300	05.87±0.3	2.61±0.4	57.1	0.54	2.48	0.0	0.009	23.0
	600 °C	SPB600	09.10±0.2	9.04±0.6	59.1	8.33	1.81	ND	0.140	32.6

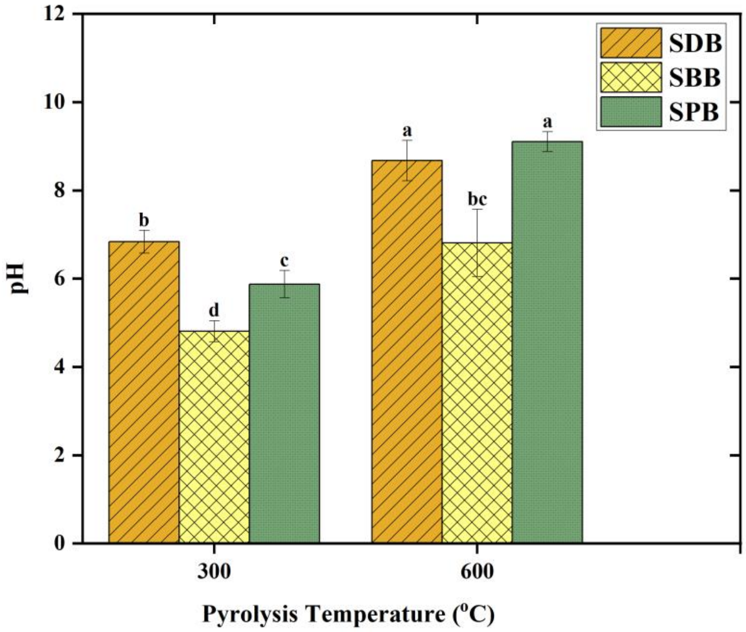

Figure 4 (a) pH of the biochar samples derived from Sawdust, Sugarcane bagasse and Soapnut pith pyrolyzed at 300°C and 600°C.

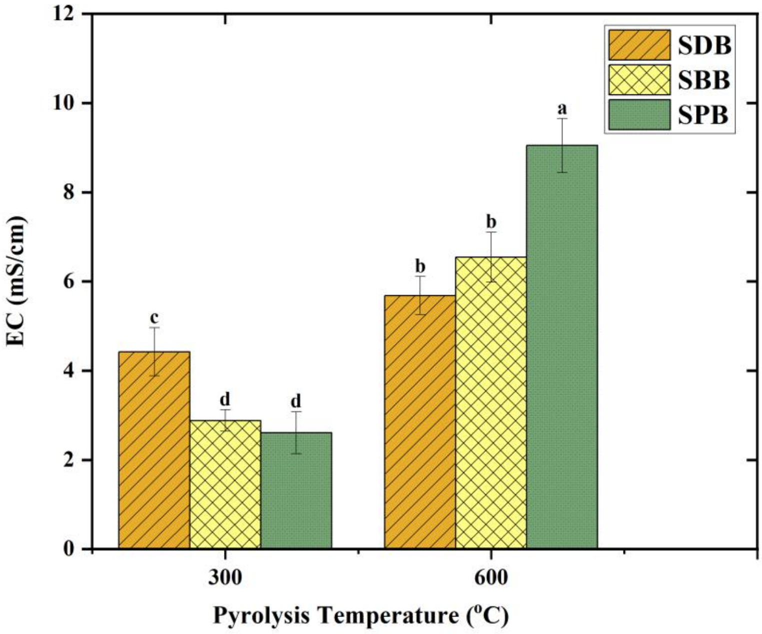

Figure 4 (b) EC (mS/cm) of the biochar samples derived from Sawdust, Sugarcane bagasse and Soapnut pith pyrolyzed at 300°C and 600°C.

In Figure 4 (b), EC results of biochar samples derived from sawdust, sugarcane bagasse, and soapnut pith are given. As the temperature increases, EC values for biochar also increase. The highest EC values were obtained in soapnut pith biochar produced at 600°C (9.04±0.6 mS/cm). Nguyen *et al.,* 2018 reported that the electrical conductivity of biochar had exhibited a strong linear correlation with the ash content ($R^2 = 0.53$, $p < 0.05$) and with the soluble salt concentration ($R^2 = 0.95$, $p < 0.05$). Therefore, differences in the EC values of different feedstock-derived biochar might be due to their ash content and soluble salt concentrations, primarily K^+, Ca^{2+}, Mg^{2+}, and Na^+ (Rehrah *et al*., 2014).

The C, H, N, and S elemental analysis result has shown the weight percentage (wt %) of each of these macronutrients in the biochar particle (Table 3). The C concentration varies from 53.5% to 75% by weight in sawdust biochars, exhibiting a 21.5% C increase in SDB600 compared to sugarcane bagasse and soapnut pith biochars. Only a 2% C increase can be observed in soapnut pith biochar. This difference in C concentration can be explained based on fixed carbon and volatile matter content. The percentage of H and N exhibit an indirect proportion among the biochar samples; that is, wt% of H was observed to be the highest in biochar prepared at 600ºC (SPB600), whereas wt% of N was high in biochar prepared at 300ºC (SPB300). This might be due to the high nutrient content in soapnut pith. The presence of S was not detected in any biochar samples. The high C content and low H/C ratio are the key indicators of the aromatic character and stability of biochar particles in soil (Domingues RR *et al*., 2017). Because of the high C content, SDB600 exhibits a minor H/C ratio (0.016) compared to SPB600 (0.140). The C/N ratio was observed to be highest in SDB600 (166.6) and lowest in SPB600 (32.6). Hence it can be concluded that the aromatic nature of biochar is associated with the rate of carbonization, dehydration reactions, and removal of O and H functional groups as charring intensifies (Lehman J. and Joseph S., 2009).

SEM-EDAX Analysis of Biochar and Feedstock

Scanning Electron Microscope Energy-dispersive X-Ray Spectroscopy (SEM-EDAX) is a potential technique for studying surface morphology and atomic percentage composition of feedstock and biochar particles. The SEM micrographs help obtain details about pore structure distribution around the biochar surface (Ozcimen and Mericboyu., 2010). The pore diameters at 2µm and 10µm resolutions are represented in fig. 5. It can be observed that the pore diameters range from 1.24-20.03(µm), 1.08-10.49(µm), 0.45-5.46(µm) in SD, SB, and SP biomasses, whereas 2.16-13.82 (µm), 0.82-10.5 (µm), 1.36-10.87 (µm), 0.87-9.17 (µm), 3.36-9.58 (µm) and 2.82-11.36(µm) in SDB300, SDB600, SBB300, SBB600, SPB300, and SPB600, respectively. The pyrolysis temperature and the heating rate affect the proportion of micropores ($d_{pore} < 2$ nm), mesopores (2 nm $< d_{pore} <$ 50 nm), and macropores ($d_{pore} > 50$ nm). At a slow heating rate, that is, ≤100 °C min^{-1}, volatiles release gently from biomass with no major change in morphology (Morin *et al*., 2016).

The feedstock sawdust (SD) possessed a maximum pore diameter, pore volume, and minimum surface area than sugarcane and soapnut pith. Fig. 6 & 7 illustrates the SEM micrographs of feedstocks and biochar. Compared to feedstocks, complex macropores with uniform distribution can be observed in all biochar particles. SDB300 exhibits maximum pore diameter (2.16-13.82 µm), pore-volume, and minimum surface area, whereas SBB600 possesses minimum pore diameter (0.87-9.17 µm), pore-volume, and maximum surface area. Instead of micropores and mesopores, a wide distribution of macropores can be observed. The pyrolysis temperature notably impacted the pore diameter and morphology of biochar. At temperatures 300 and 600°C, a significant amount of volatile matter gets expelled from the biomass, resulting in the pore opening. At 600°C, the loss of only a relatively small fraction of volatile matter caused the development of porosity and the occurrence of structural shrinkage and pore narrowing. These variations among the biochar will result in a different capacity to adsorb soluble inorganic and organic matter, gas molecules, and nutrients in the soil matrix and provide a habitat for microbial communities to colonize, grow, and reproduce (Sainju *et al*., 2006). According to Di Blasi 2009, mesopores and macropores are significant contributors to the reactive surface area, while the less accessible micropores barely participate in the reaction.

Fig. 8 and table 4 depict the distribution of atomic percentage composition of inorganic elements present in the feedstock biomass and biochar. The atomic C content in feedstock was found to be decreased in the order SP (81%)> SD (67.39%)> SB (61.53%), whereas, in biochar, the increase is visible. The high-temperature biochar such as SBB600 and SDB600 possessed high atomic C. The observed differences can be explained based on their ash content. The atomic Si was present only in SDB600, SBB300, SBB600, and SPB600. Si typically exists in the form of phytoliths that protect plant C from degradation (Wilding, 1967; Krull *et al*., 2003; Smith and white., 2004; Parr and Sullivan., 2005; Parr., 2006). The atomic percentage of oxygen was decreased in biochar samples prepared at 300 and 600^{o}C compared to raw feedstock. This atomic percentage was associated with the dehydration reaction and removal of oxygen and hydrogen atoms as charring progresses. During the pyrolysis, carbon and inorganic elements were enriched in biochar.

The results imply that most of the inorganic elements such as Ca, K, P, Mg, and Si are barely released during the pyrolysis of feedstock, as indicated in the previous work by Anca-Couce *et al*., 2017. With increasing the pyrolysis temperature from 300 to 600°C, Al, S, Cl, and Cu concentrations did not show a significant trend. A higher atomic concentration of C, K, P, Ca, and Mg were detected from biochar produced at a higher temperature. The sudden increase in atomic K concentration in the sawdust, sugarcane bagasse, and soapnut pith biochars produced at a pyrolysis temperature of 300 and 600°C may be the cause of the slightly higher reactivity in comparison with the raw feedstock. Ca is the most common inherent inorganic element in woody biomass, usually followed by varying contents of K, Si, Mg, and P and a trace amount of S and Cl. A previous study (Asadullah, M. *et.al*., 2010) showed that biochar or charcoal reactivity is mainly affected by three parameters: (i) the content and composition of inorganic elements, (ii) the physical structure, that is, the specific surface area and pore-size distribution, and (iii) the content of functional groups and chemical structure of the carbon matrix. Therefore, a certain amount of inorganic elements retained in the biochar can influence their reactivity and catalytic role even in the soil system upon application as an amendment. The alkaline nature of biochar will facilitate the cation exchange capacity and potentially serve as a slow-release source of plant nutrients (Limwikran *et al*., 2018).

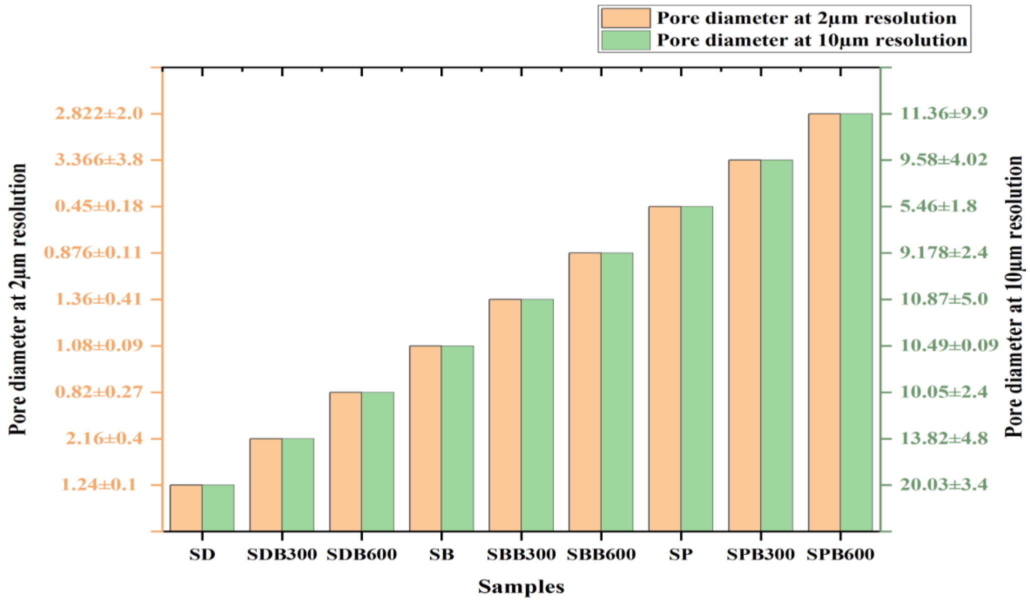

Figure 5. Double Y Column of the pore diameter in feedstock and biochar samples at 2µm and 10µm resolutions.

Table 4. Atomic composition of inorganic elements in the feedstock and biochar samples

Samples	Atomic (%) Composition of Inorganic Elements										
	C (%)	O (%)	Mg (%)	Al (%)	S (%)	P (%)	K (%)	Ca (%)	Cl (%)	Si (%)	Cu (%)
Sawdust	67.39	32.4	0.04	0.07	0.04	0.03	0.03	-	-	-	-
SDB300	77.4	22.1	-	-	-	0.08	0.19	0.23	-	-	-
SDB600	87.91	9.09	0.21	-	-	0.26	0.28	2.04	0.19	0.01	-
Sugarcane Bagasse	61.53	38.33	-	-	-	0.04	-	0.06	0.05	-	-
SBB300	87.9	11.36	-	-	-	-	0.39	-	-	0.34	-
SBB600	93.88	5.29	-	-	0.08	0.07	0.32	-	0.11	0.26	-
Soapnut Pith	81.00	19.00	-	-	-	-	-	-	-	-	-
SPB300	80.15	19.65	0.04	-	-	-	0.15	-	-	-	-
SPB600	78.37	18.24	0.58	0.36	0.09	0.29	1.17	0.75	-	0.13	0.01

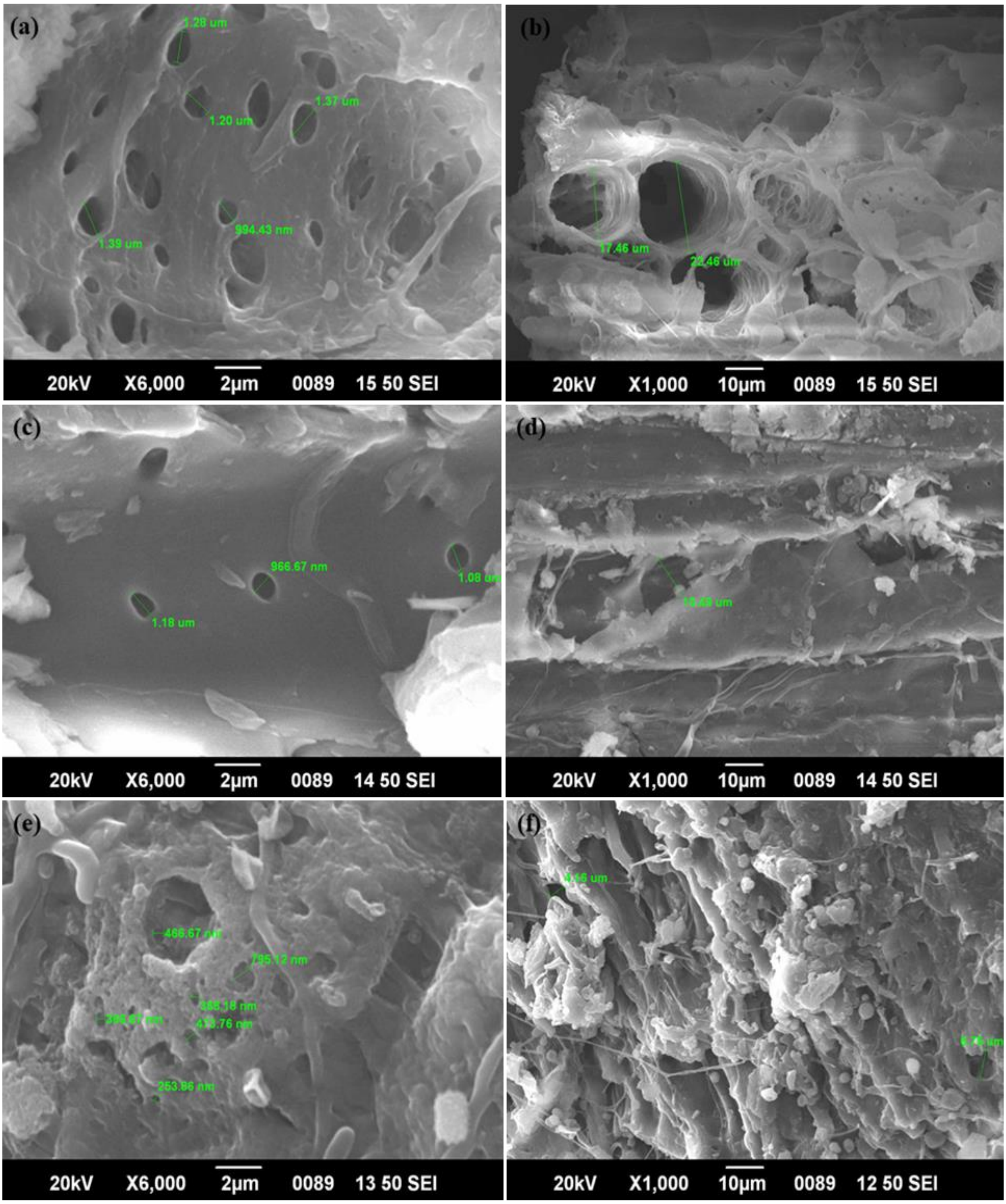

Figure 6. SEM Micrographs of ligno-cellulosic biomasses such as Sawdust (a,b), Sugarcane bagasse(c,d), and Soapnut pith (e,f) at 2µm and 10µm resolutions.

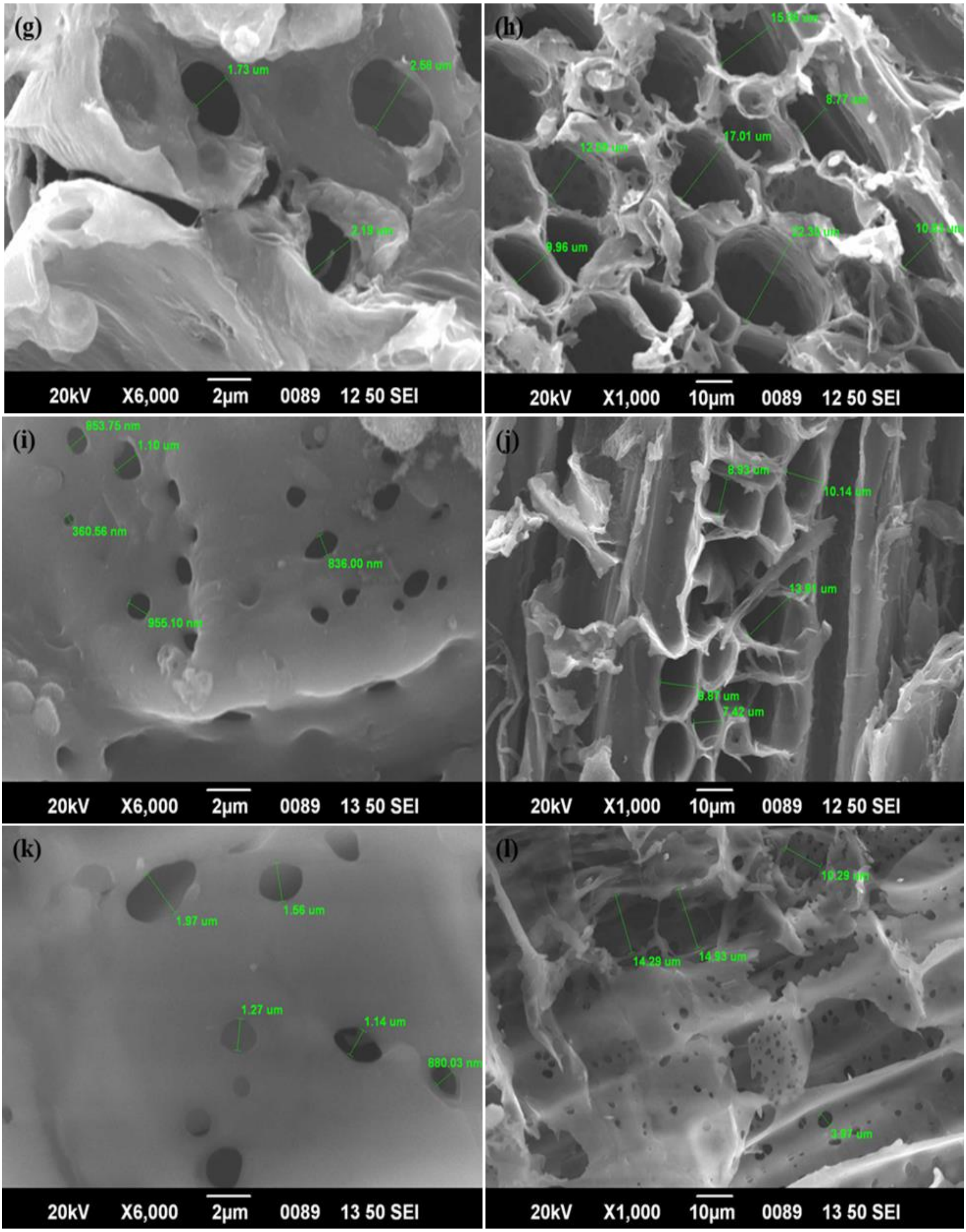
(g)
1.73 um
2.58 um
2.19 um
20kV X6,000 2µm 0089 12 50 SEI
(h)
17.01 um
8.77 um
9.96 um
22.30 um
20kV X1,000 10µm 0089 12 50 SEI
(i)
853.75 nm
1.10 um
360.56 nm
836.00 nm
955.10 nm
20kV X6,000 2µm 0089 13 50 SEI
(j)
8.93 um
10.14 um
8.87 um
7.42 um
20kV X1,000 10µm 0089 12 50 SEI
(k)
1.97 um
1.56 um
1.27 um
1.14 um
880.03 nm
20kV X6,000 2µm 0089 13 50 SEI
(l)
10.29 um
14.29 um
14.93 um
3.97 um
20kV X1,000 10µm 0089 13 50 SEI

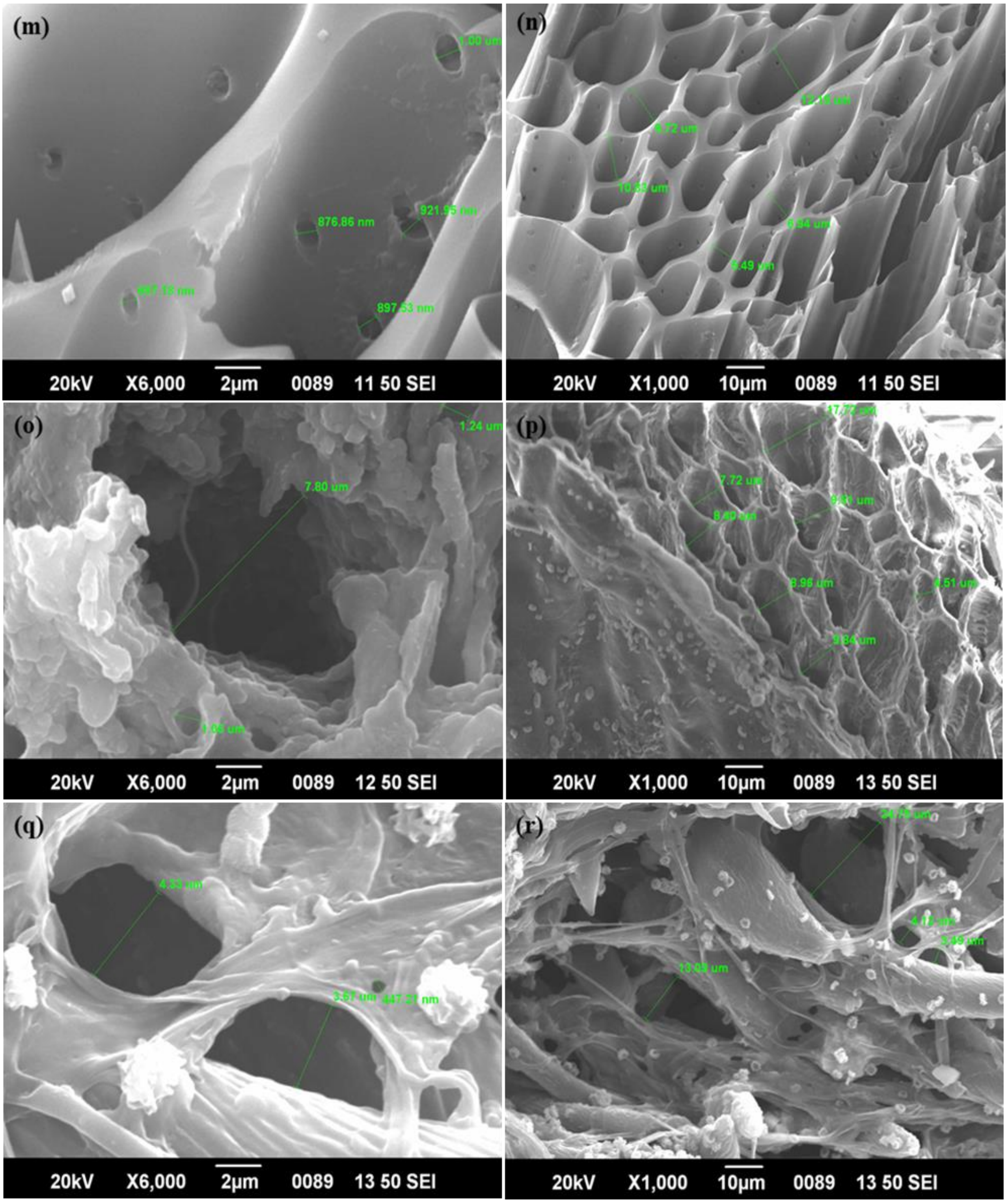

Figure No.7. SEM Micrographs of biochar samples produced at 300oC and 600oC; SDB300(g,h), SDB600 (i,j), SBB300 (k,l), SBB600 (m,n), SPB300 (o,p), and SPB600 (q,r) at 2µm and 10µm resolutions.

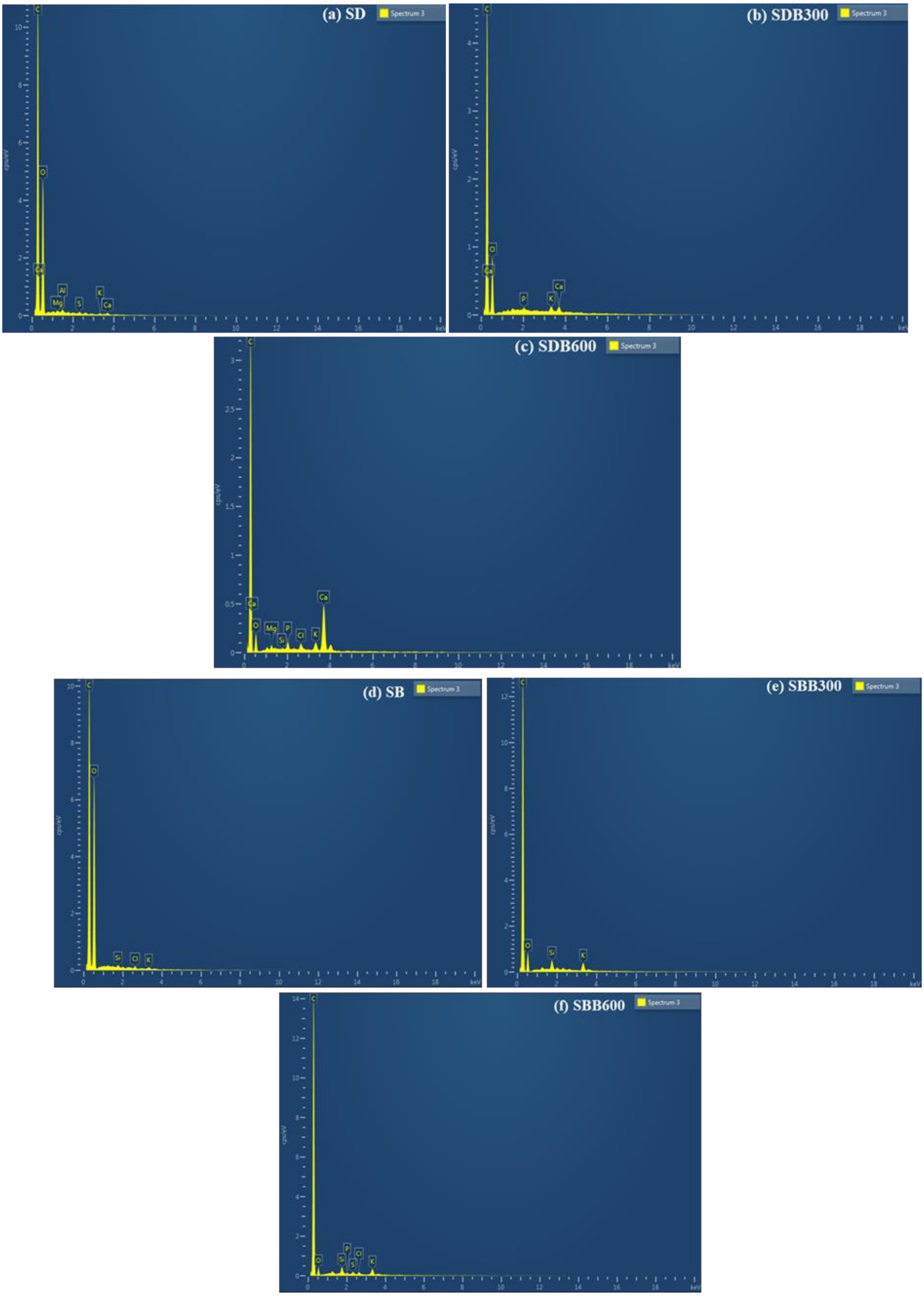
(a) SD
Spectrum 3
C
O
Ca
Al
Mg
S
K
Ca
cps/eV
keV
(b) SDB300
Spectrum 3
C
O
Ca
P
K
Ca
cps/eV
keV
(c) SDB600
Spectrum 3
C
Ca
O
Mg
Si
P
Cl
K
Ca
cps/eV
keV
(d) SB
Spectrum 3
C
O
Si
Cl
K
cps/eV
keV
(e) SBB300
Spectrum 3
C
O
Si
K
cps/eV
keV
(f) SBB600
Spectrum 3
C
O
Si
P
S
Cl
K
cps/eV
keV

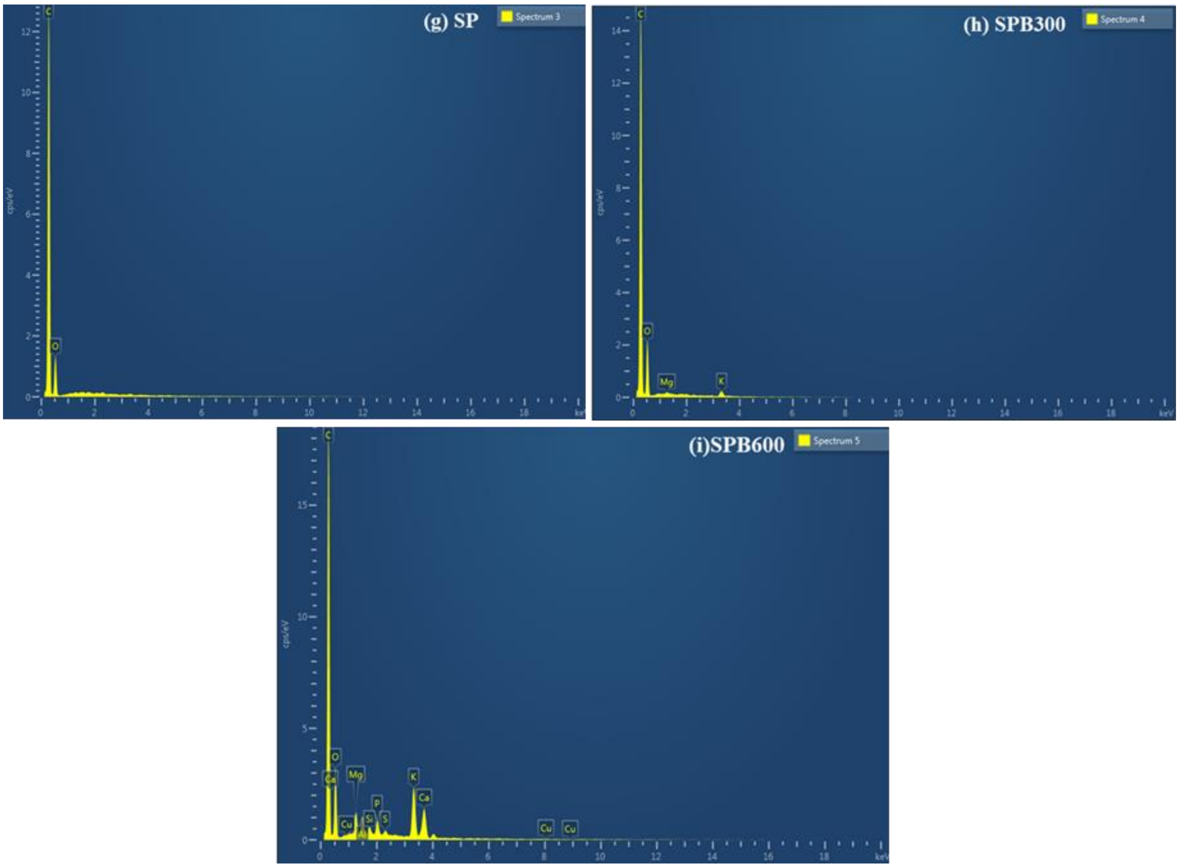

Figure No.8. EDAX spectra of SD (a), SDB300 (b), SDB600 (c), SB (d), SBB300 (e), SBB600 (f), SP (g), SPB300 (h), SPB600 (i).

Conclusions

This study investigated the biochar's possible physical, chemical, and morphological advancement from three different ligno-cellulosic biomass materials: hardwood sawdust, sugarcane bagasse, and soapnut pith of *Sapindus trifoliatus* native to Kerala. This study also aimed to put forward a better biochar supplement for cultivable soil as a supplement, a suitable adsorbent for environmental remediation purposes based on their characteristic features. The feedstock type and pyrolysis conditions significantly impact biochar's proximate, ultimate, and surface morphological properties. The fixed carbon increased as pyrolysis intensified. The VM/FC ratio of 1.09±2.3 showed sawdust biochar's stable and aromatic nature (SDB600). The pH was found to be alkaline. The feedstock's nitrogen content was most conserved in low-temperature biochars (SDB300, SBB300, and SPB300). The macropores distributed over the biochar surface enhance the surface area, making it a suitable adsorbent and providing a habitat for soil micro-organisms to thrive. Among the three sets of biochars prepared from the sawdust, sugarcane bagasse, and soapnut pith biomass at 300 and 600^{o}C, SDB600 was the best biochar for stability and fixed C content. Hence it can be recommended for soil supplementation purposes. The SBB600 contained numerous macropores (>50 nm) over their surface and could be a suitable adsorbent for environmental remediation applications compared to the biochar of sawdust and sugarcane bagasse origin. The recommendations made from the study need to be tested by supplementing selected biochar materials in the soil. Meanwhile, the conversion of this selected ligno-cellulosic biomass to biochar is a sustainable approach for environmental management.

Acknowledgement

The authors acknowledge the research scheme National Fellowship for Scheduled Caste (NFSC) belongs to University Grants Commission (UGC) for financial support. The authors acknowledge the Sophisticated Test and Instrumentation Center (STIC), Cochin University of Science and Technology (CUSAT) and Inter-University Instrumentation Centre (IUIC), Mahatma Gandhi University, Kottayam for providing the analytical facilities.

Funding

This work was funded by the University Grants Commission (UGC) under the research scheme of National Fellowship for Scheduled Caste (NFSC) [grant numbers: 43202/ (NET-DEC 2018)].

References

Agusalim Masulil, 2010., Rice Hulk biochar for rice-based cropping system in Acid soil, the Characteristics of rice husk biochar, and its influence on the properties of acid sulfate soils. and rice growth in west Kalimantan, Indonesia. J. Agricultural.sci., 2:39-47.

Agusalim Masulili, Wani Hadi Utomo and Erwin I Wisnubroto, 2016. Growing Rice (Oriza sativa L.) in the Sulphate Acid Soils of West Kalimantan, Indonesia. International Journal of Agricultural Research, 11: 13-22.10.3923/ijar.2016.13.22.

Anca-Couce, A.; Dieguez-Alonso, A.; Zobel, N.; Berger, A.; Kienzl, N.; Behrendt, F. Influence of Heterogeneous Secondary Reactions during Slow Pyrolysis on Char Oxidation Reactivity of Woody Biomass. Energy Fuels 2017, 31, 2335– 2344. 10.1021/acs.energyfuels.6b02350.

Anonymous. Publication and Informative Directorate. CSIR, New Delhi, 1988, pp. 87-88.

Asadullah, M.; Zhang, S.; Min, Z.; Yimsiri, P.; Li, C.-Z. Effects of biomass char structure on its gasification reactivity. Bioresour. Technol. 2010, 101, 7935– 7943. 10.1016/j.biortech.2010.05.048.

Chopra RN, Nayar SL and Chopra IC. CSIR Publication, New Delhi, 1956.

Crombie Kyle, Ondřej Mašek, Saran P. Sohi, Peter Brownsort, Andrew Cross (2013). The effect of pyrolysis conditions on biochar stability as determined by three methods. GCB Bioenergy (2013). Pages: 5, 122-131. https://doi.org/10.1111/gcbb.12030.

Di Blasi, C. Combustion and gasification rates of lignocellulosic chars. Prog. Energy Combust. Sci. 2009, 35, 121– 140.10.1016/j.pecs.2008.08.001.

Domingues Rimena R., Paulo F. Trugilho, Carlos A. Silva, Isabel Cristina N. A. de Melo, Leônidas C. A. Melo, Zuy M. Magriotis, Miguel A. Sánchez-Monedero (2017). Properties of biochar derived from wood and high-nutrient biomasses with the aim of agronomic and environmental benefits. https://doi.org/10.1371/journal.pone.0176884.

Duchan V, Kopar T (2001) Sawdust and paper-making sludge as pore-forming agents for lightweight clay bricks source. Ind Ceram 21(2):81–86.

Edeoga HO, Omosun G and Uche LC. Afri J Biotechnol 2006; 5(10): 892-895.

H.Demir, A. Top, D.Balköse and S.Ülkü (2008). Dye adsorption behavior of Luffa cylindrica fibers. Journal of Hazardous Materials. Volume 153, Issues 1–2, 1 May 2008, Pages 389-394. https://doi.org/10.1016/j.jhazmat.2007.08.070.

Haijun Sun., Haiying Lu., Lei Chu., Hongbo Shao., Weiming Shi (2017). Biochar applied with appropriate rates can reduce N leaching, keep N retention and not increase NH_3 volatilization in a coastal saline soil. Science of The Total Environment Volume 575, 1 January 2017, Pages 820-825. https://doi.org/10.1016/j.scitotenv.2016.09.137.

Horisawa Sakae., Masahide Sunagawa., Yutaka Tamai Yuki Matsuoka., Tohru Miura., Minoru Terazawa (1999). Biodegradation of non-lignocellulosic substances II: physical and chemical properties of sawdust before and after use as artificial soil. J Wood Sci (1999) 45:492-497. © The Japan Wood Research Society 1999.

Jeff Novak and W. J. Busscher (2013). Selection and Use of Designer Biochars to Improve Characteristics of Southeastern USA Coastal Plain Degraded Soils. Advanced Biofuels and Bioproducts.10.1007/978-1-4614-3348-4-7.

Jindo K., H. Mizumoto·, Y. Sawada., M. A. Sanchez-Monedero., and T. Sonoki (2014). Physical and chemical characterization of biochars derived from different agricultural residues. Biogeosciences, 11, 6613–6621, 2014. https://doi.org/10.5194/bg-11-6613-2014.

Keiluweit Marco., Peter S. Nico., Mark G. Johnson., and Markus Kleber (2010). Dynamic Molecular Structure of Plant Biomass-Derived Black Carbon (Biochar). Environ. Sci. Technol. 2010, 44, 4, 1247–1253. https://doi.org/10.1021/es9031419.

Krull, E.S., Skjemstad, J.O., Graetz, D., Grice, K., Dunning, W., Cook, G., Parr, J.F. (2003). 13C depleted charcoal from C4 grasses and the role of occluded carbon in phytoliths. Organic Geochemistry 34:1337-1352.

Lehman, J. and Joseph, S. 2009. Biochar for environmental management: An introduction. In: J. Lehman and S. Joseph edited. Biochar. Published online. Assessed 30.06.2016.

Lewandowski, I. and Kicherer, A. (1997) Combustion Quality of Biomass: Practical Relevance and Experiments to Modify the Biomass Quality of Miscanthus x giganteus. European Journal of Agronomy, 6, 163-177. https://doi.org/10.1016/s1161-0301(96)02044-8.

Limwikran T., I. Kheoruenromne., A. Suddhiprakarn., N. Prakongkep., R.J. Gilkes (2018) Dissolution of K, Ca, and P from biochar grains in tropical soils, Geoderma, Volume 312, 2018, Pages 139-150, ISSN 0016-7061.https://doi.org/10.1016/j.geoderma.2017.10.022.

Limwikran, T., Kheoruenromne, I., Suddhiprakarn, A., Prakongkep, N., & Gilkes, R. J. (2018). Fertility Capability and Responses of Oxisols to Agricultural Wastes Biochar Application. Thai Journal of Agricultural Science, 51(1), 42-54.

Low N.M.P., Fazio, P., and Guite, P. (1984). Development of lightweight insulating clay products from the clay sawdust-glass system. Ceramics International, 10(2), 59-65.

Maiti S. K. 2003. Handbook of Methods in Environmental Studies. Volume 2. ABD publishers, 110-121.

Maiti S. K. 2003. Handbook of Methods in Environmental Studies. Volume 2. ABD publishers, 110-121.

McMichael Anthony J, John W Powles, Colin D Butler, Ricardo Uauy (2007). Food, livestock production, energy, climate change, and health. Lancet 2007; 370: 1253–63. 10.1016/S0140-6736(07)61256-2.

Melo Leônidas C., Aline Renee Coscione., Cleide Aparecida Abreu., Aline Peregrina Puga., and Otávio Antonio Camargo (2013). Influence of Pyrolysis Temperature on Cadmium and Zinc Sorption Capacity of Sugar Cane Straw–Derived Biochar.

Morin, M.; Pécate, S.; Hémati, M.; Kara, Y. Pyrolysis of biomass in a batch fluidized bed reactor: Effect of the pyrolysis conditions and the nature of the biomass on the physicochemical properties and the reactivity of char. J. Anal. Appl. Pyrolysis 2016, 122, 511– 523.10.1016/j.jaap.2016.10.002.

Mukherjee, a., A.R. Zimmerman and W. Harris. 2011. Surface chemistry variations among a series of laboratory- produced biochars. Geoderma 163:247-255.

Nguyen, Loc X., Phuong T. M. Do., Chiem H. Nguyen., Ryota Kose., Takayuki Okayama., Thoa N. Pham., Phuong D. Nguyen., and Takayuki Miyanishi (2018). Properties of Biochars Prepared from Local Biomass in the Mekong Delta, Vietnam. Bioresources.10.15376/biores.13.4.7325-7344.

Novak, Jeffrey M.1; Busscher, Warren J.1; Laird, David L.2; Ahmedna, Mohamed3; Watts, Don W.1; Niandou, Mohamed A. S.3 Impact of Biochar Amendment on Fertility of a Southeastern Coastal Plain Soil, Soil Science: February 2009 - Volume 174 - Issue 2 - p 105-112. 10.1097/SS.0b013e3181981d9a.

Özçimen Didem and Ayşegül Ersoy-Meriçboyu (2010). Characterization of biochar and bio-oil samples obtained from carbonization of various biomass materials. Renewable energy, 2010, vol. 35, issue 6, 1319-1324.10.1016/j.renene.2009.11.042.

Parr, J.F. (2006). Effect of fire on phytolith coloration. Geoarchaeology, 21(2): 171-185.

Parr, J.F., Sullivan, L.A. (2005). Soil carbon sequestration in phytoliths. Soil Biology and Biochemistry, 37 (1), 117-124.

Rainer Janu., Verena Mrlik ., Doris Ribitsch ., Jakub Hofman ., Petr Sedláček ., Lucie Bielská ., Gerhard Soja (2021). Biochar surface functional groups as affected by biomass feedstock, biochar composition and pyrolysis temperature. Carbon Resources Conversion Volume 4, 2021, Pages 36-46. https://doi.org/10.1016/j.crcon.2021.01.003.

Rajkovich Shelby & Akio Enders & Kelly Hanley & Charles Hyland & Andrew R. Zimmerman & Johannes Lehmann (2011). Corn growth and nitrogen nutrition after additions of biochars with varying properties to temperate soil. Biol Fertil Soils (2012) 48:271–284.10.1007/s00374-011-0624-7.

Rehrah, D., Reddy, M. R., Novak, J. M., Bansode, R. R., Schimmel, K. A., Yu, J., Watts, D. W., and Ahmedna, M. (2014). "Production and characterization of biochars from agricultural byproducts for use in soil quality enhancement," J. Anal. Appl. Pyrol. 108, 301-309.10.1016/j.jaap.2014.03.008.

Robber JM and Tyler VS. Williams and Wilkins, Baltimore, 1996, pp.1 -14.

Sadaka S, Sharara MA, Ashworth A, Keyser P, Allen F, Wright A (2014) Characterization of biochar from switchgrass carbonization. Energies 7:548–567.10.3390/en7020548.

Sadaka, Sammy & Sharara, Mahmoud & Ashworth, Amanda & Keyser, Patrick & Allen, Fred & Wright, Andrew. (2014). Characterization of Biochar from Switchgrass Carbonization. energies 1996-1073. 7. 548-567. 10.3390/en7020548.

Sainju, Upendra M., Bharat P. Singh., Wayne F. Whitehead., and Shirley Wang (2006). Carbon Supply and Storage in Tilled and Nontilled Soils as Influenced by Cover Crops and Nitrogen Fertilization. J. Environ. Qual. 35:1507–1517 (2006). https://doi.org/10.2134/jeq2005.0189.

Smith Francesca A.., and James W.C.White (2004). Modern calibration of phytolith carbon isotope signatures for C_3/C_4 paleograssland reconstruction. Palaeogeography, Palaeoclimatology, Palaeoecology Volume 207, Issues 3–4, 20 May 2004, Pages 277-304. https://doi.org/10.1016/j.palaeo.2003.09.029.

Tsai, W.-T. (2017). "The potential of pyrolysing exhausted coffee residue for the production of biochar," in: Handbook of Coffee Processing By-Products: Sustainable Application, C. M. Galanakis (ed.), Academic Press, Cambridge, MA, pp. 299-322.

Urum K and Pekdemir T. Chemosphere 2004; 57(9): 1139-1150.

Wei Siye, Mengbo Zhu, Jianzhong Song, Ping'an Peng (2017). Comprehensive Characterization of Biochars Produced from Three Major Crop Straws of China. Vol 12, No 2 (2017).

Wilding L.P. (1967). Radiocarbon dating of biogenetic opal. Science Vol 156, Issue 3771, pages: 156:66–67.10.1126/science.156.3771.66.

Yu Chun-Hui., Shan-Li Wang, Prapasiri Tongsiri., Mei-Ping cheng and Hung Yu Lai., (2018). Effects of poultry litter Biochar on soil properties and growth of water spinach (Ipomoea aquatic Forsk). Sustainability 10(7):2536.10.3390/su10072536.

Zhao, Shi-Xiang & Yu, Xiao-Ling & Li, Zhong-Hui & Yang, Yan & Zhang, Xia & Wang, Xu-Dong & Zhang, Afeng. (2017). Effects of Biochar Pyrolyzed at Varying Temperatures on Soil Organic Carbon and Its Components: Influence on the Composition and Properties of Humic Substances. Huan jing ke xue= Huanjing kexue / [bian ji, Zhongguo ke xue yuan huan jing ke xue wei yuan hui "Huan jing ke xue" bian ji wei yuan hui.]. 38. 769-782. 10.13227/j.hjkx.201604059.